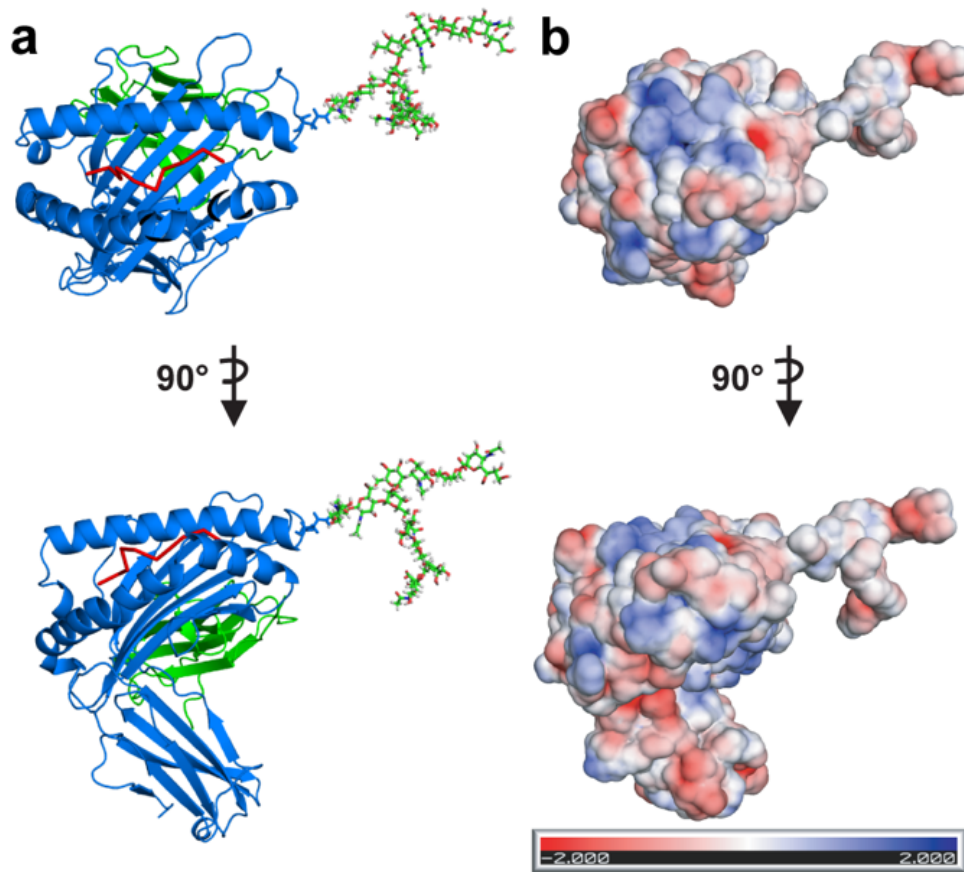
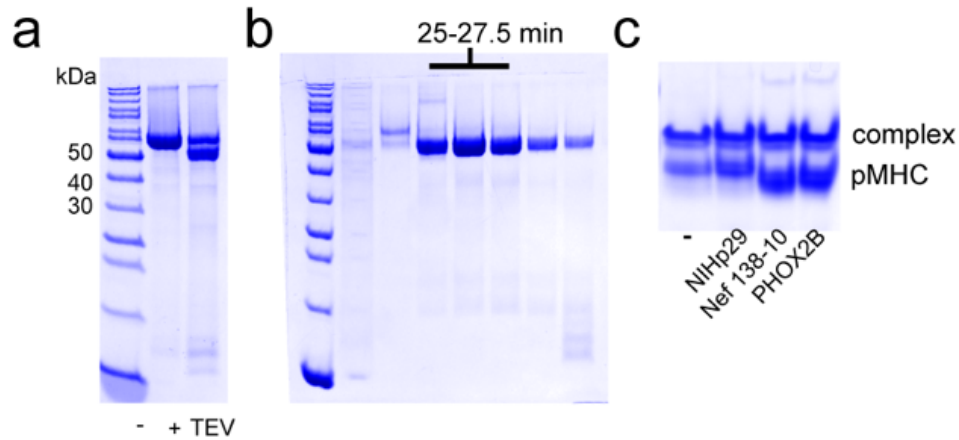


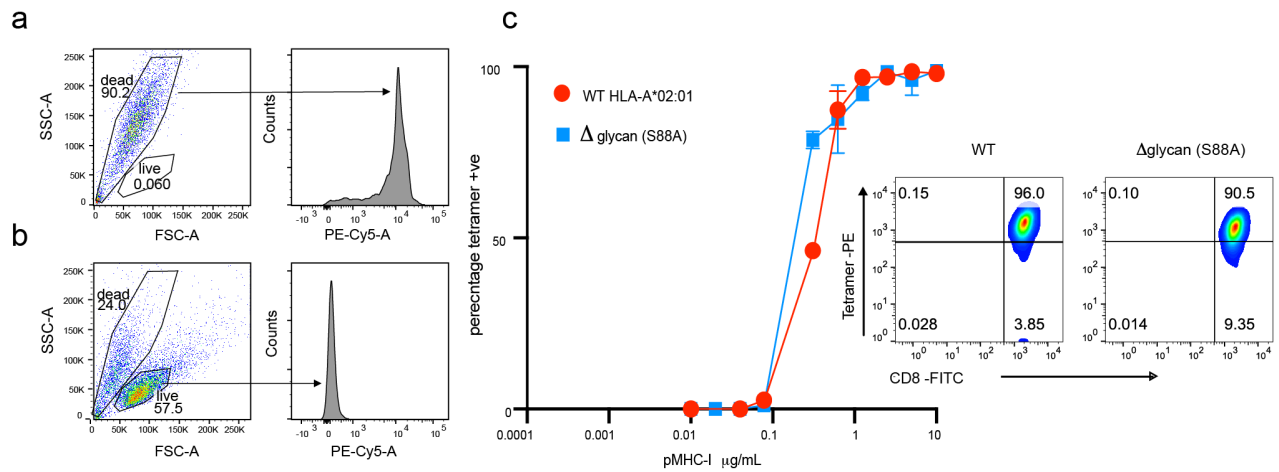
Supplementary Figures



Supplementary Figure S1. Structure modeling of the glycan moiety on the conserved Asn 86 residue. (a) HLA-A*02:01 in complex with the heteroclitic MART-1 peptide (PDB ID: 1JF1) modelled to show a biantennary di-sialylated glycan at position N86. The heavy chain is colored blue, $\beta 2m$ green, MART-1 peptide, red. (b) Electrostatic surface representation of the MHC-I molecule and glycan from the top view and side view. Solvent-accessible surface representation with electrostatic potential in the indicated ranges ($-2 \text{ kcal}/(\text{mol}\cdot e)$ in red to $+2 \text{ kcal}/(\text{mol}\cdot e)$ in blue) were calculated using CHARMM-GUI. All calculations were performed at 150 mM ionic strength, 298 Kelvin, pH 7.2, protein dielectric 2.0, and solvent dielectric 78.54. Electrostatic potentials are given in units of kT/e . A 1.4 \AA solvent (probe) radius and $10.0 \text{ points}/\text{\AA}^2$ density was used to calculate molecular surfaces.



Supplementary Figure S2. Analysis of HLA-A*24:02/TAPBPR leucine-zippered complex. (a) Streptactin-purified complex was TEV digested and electrophoresed on a 12% SDS PAGE gel prior to size exclusion chromatography (SEC) (b) Gel electrophoresis of complex eluted from an SEC S200 16/300 increase column (50mM Tris, 100mM, NaCl, running at a rate of 0.5mL/min). The complex peak (25-27.5min) was collected. (c) Native gel electrophoresis of HLA-A*24:02/TAPBPR complex dissociation in the presence of relevant high affinity peptides (Nef 138_10 and PHOX2B) and irrelevant peptide (NIHp29).



Supplementary Figure S3. Flow cytometry analysis. (a) DMF5 cells are a HLA-A*02:01 restricted human lymphocyte line that express both the MART-1 specific TCR and CD8 co-receptor. For flow cytometry, dead-cells (PE-Cy5-A channel) were identified by treatment with ethanol followed by propidium iodide staining (b) Live singletons were selected by forward and side light scattering properties. The percentage of total population within each gate is indicated. (c) Titration of PE- HLA-A*02:01 MART-1 (WT) -and Δ glycan (S88A) tetramers on DMF5 by flow cytometry with inset, 1.25 $\mu\text{g/mL}$ tetramer, 1 $\mu\text{g/mL}$ anti-human CD8-FITC (BD San Jose).

Table S1. Previously described epitopic peptides used in this study

Peptide	Sequence	Length	predicted IC50 (nM) HLA-A*02:01	predicted IC50 (nM) HLA-A*68:02	predicted IC50(nM) HLA-A*24:02
TAX9	LLFGVPVYV	9	3.4	64	-
NY-ESO-1	SLLMWITQA	9	23	7297	-
GM1	GLLGIGILTV	10	15.9	12160.2	-
GM2	ETAGVPADV	9	14820.3	5.3	-
GM3	ETAGIGILTV	10	4436.9	4.4	-
GM4	GLLGVPLYV	9	5.4	4662.9	-
NIH p29	YPNVNIHNF	9	22457.6	13418.9	-
P18_I10	RGPGRAFVFI	10	17132.2	12829.9	-
MART-1	EAAGIGILTV	10	5322.6	-	-
PHOX2B	VYGFVRACL	9	-	-	466.54
Nef138-10	RYPLTFGWCF	10	-	-	6.57

* All predictions of IC50 values were made using NetMHCpan 4.0; Jurtz,V., Paul,S., Andreatta,M., Marcatili,P., Peters,B. and Nielsen,M. (2017) *J. Immunol. Baltim. Md 1950*, **199**, 3360–3368.

Table S2. SARS-CoV-2 epitopic peptides used in this study

Swiss-Model Repository Reference	Sequence	Length	predicted IC50 (nM) HLA:A*02:01*	Structure-Based Model**	charge
YP_009724390.1	ALNTLVKQL	9	1633.23	Weak binder	+1
YP_009724390.1	VLNDILSRL	9	33.57	Strong binder	0
YP_009724390.1	RLNEVAKNL	9	940.92	Strong binder	+1
YP_009724390.1	NLNESLIDL	9	177.32	Strong binder	-2
YP_009724390.1	FIAGLIAIV	9	10.29	Strong binder	0
YP_009724392.1	GLMWLSYFI	9	3.87	Strong binder	0
YP_009724392.1	LLLDRLNQL	9	14.81	Strong binder	0
YP_009724389.1	GMSRIGMEV	9	50.61	Strong binder	0
YP_009724389.1	WLMWLIINL	9	6.60	Weak binder	0
YP_009724389.1	ILLLDQALV	9	27.11	Strong binder	0
YP_009724389.1	SLPGVFCGV	9	24.07	Strong binder	-1
YP_009724393.1	TLACFVLA AV	10	20.28	Strong binder	0
YP_009724390.1	KLPDDFTGCV	10	77.11	Strong binder	-1

* Using NetMHCpan 4.0; Jurtz, V., Paul, S., Andreatta, M., Marcatili, P., Peters, B. and Nielsen, M. (2017) *J. Immunol. Baltim. Md 1950*, **199**, 3360–3368.

**Classified according to *Rosetta* binding energies, as outlined in; Nerli, S. and Sgourakis, N.G. (2020) *bioRxiv*, 2020.03.23.004176.